



## Structure inhibited pit initiation in a Ni–Nb metallic glass

Z.M. Wang, J. Zhang, X.C. Chang, W.L. Hou, J.Q. Wang\*

Shenyang National Laboratory for Materials Science, Institute of Metal Research, CAS, Shenyang 110016, PR China

### ARTICLE INFO

#### Article history:

Received 7 September 2009

Accepted 7 December 2009

Available online 30 December 2009

#### Keywords:

A. Alloy

A. Glass

C. Amorphous structures

C. Interfaces

C. Passive films

C. Pitting corrosion

### ABSTRACT

A model metallic glass Ni<sub>50</sub>Nb<sub>50</sub>, which would undergo a polymorphous transformation during devitrification, was selected to clarify the correlation of amorphous structure with corrosion. The electrochemical polarization behaviour, film breakdown and composition of surface film have been studied in detail by comparing the amorphous alloy with its crystalline counterparts. Interestingly, it was found that the pit initiation is inhibited greatly on amorphous sample relative to the crystallized one. The origin is thought to be related to the defective interface beneath passive film that inhibits the formation of pitting precursors in corrosion.

© 2009 Elsevier Ltd. All rights reserved.

### 1. Introduction

It is well known that metallic glasses with their unique structure possess excellent mechanical, magnetic and chemical properties [1]. The corrosion properties of metallic glasses have been studied extensively since the discovery of highly corrosion-resistant Fe–Cr–metalloid metallic glasses in the 1970s [2,3]. It has been noticed that the corrosion resistance of metallic glasses is much sensitive to their chemical composition. For example, some Fe- and Ni-based metallic glasses exhibit high corrosion resistance and are immunized from pitting corrosion even at concentrated HCl solutions [3,4], while most of the Mg- and Cu-based metallic glasses cannot be passivated in Cl<sup>-</sup> bearing solutions [5]. Further, minor additions of alloying elements to metallic glasses can produce significant influences on their corrosion behaviour [6,7]. Correspondingly, the compositional homogeneity and the high solubility were regarded as dominant factors in influencing the corrosion resistance of metallic glasses.

It is worthy of noting that the amorphous structure itself could affect the corrosion of metallic glasses, but the understanding of such an effect is still unclear. Comparative studies on some multi-component metallic glasses, such as FeZrNbB(Cu) [8], CrNiP [9] and ZrCuNiAlTi [10], suggested that the presence of crystalline phases would decrease their corrosion resistance. However, they exhibited no distinct difference in corrosion resistance for other metallic glasses, e.g. ZrTiCuNiBe [11], AlNiY [12] and NiNbTiZrCoCu [13], as compared with their partially or fully crystallized counter-

parts. Normally, multi-component metallic glasses would undergo compositional redistributions with the formation of precipitated crystalline phases upon devitrification. In these systems, the diversity in composition, size and chemical activity of the precipitated crystalline phases obscures the structural effect [9]. Thus, to clarify the intrinsic structural effect on corrosion of metallic glasses, excluding the compositional effect by proper selection of model alloy system becomes premier.

As for the structural effect on corrosion of metallic glasses, it is closely associated with dissolution, passivation as well as durability of passive film. Passive films are easily formed on metallic glasses since the alloy dissolves rapidly inducing a fast accumulation of passivating elements [3,5], and such surfaces are argued to be susceptible to localized corrosion [5]. However, little is known about the correlation between the metastable amorphous structure and the stability of passive film. Previous studies have pointed out that liquid gallium was more resistant to passivity breakdown relative to its crystalline state, resulting from the inhibition effect of liquid structure on vacancy condensation at the oxide/metal interface [14]. Such defects are believed to be an important origin for pit initiation [15–17]. It is interesting that amorphous structure with a large amount of free volume could also prevent the presence of stable vacancies and their condensation to voids [18] at the oxide/metal interface. Thus, it probably declines the risk of localized rupture of the passive film [19,20]. It is clear that a comparison between amorphous and crystalline structure correlating with the stability of passive film is highly needed.

Our aims are to make an attempt to understand how structure influences the corrosion behaviour of metallic glasses, especially on the stability of passive film. In the present paper, a Ni<sub>50</sub>Nb<sub>50</sub>

\* Corresponding author. Tel./fax: +86 24 2397 1902.

E-mail address: [jqwang@imr.ac.cn](mailto:jqwang@imr.ac.cn) (J.Q. Wang).

metallic glass was selected as a model system due to two considerations. Firstly, the  $\text{Ni}_{50}\text{Nb}_{50}$  metallic glass can transform to its crystalline state *via* polycrystallization without compositional redistribution [21]. Moreover, the nature of easily forming strongly-protective surface film and the simple components of the alloy are beneficial in the breakdown control of passive film and chemical analysis of surface/interface. Thus, to clarify the correlation of amorphous structure with corrosion, we have examined the breakdown behaviour of passive films of the model alloys, as well as the characteristics of surface film and underlying interface. Apparent inhibiting effects of corrosion failures associated with amorphous structure are characterized.

## 2. Experimental details

A  $\text{Ni}_{50}\text{Nb}_{50}$  master alloy was prepared by melting appropriate amount of pure Ni (99.96%) and Nb (99.9%) in a vacuum arc furnace under argon atmosphere. Amorphous  $\text{Ni}_{50}\text{Nb}_{50}$  ribbons with 2 mm width and about 40  $\mu\text{m}$  thickness were produced by melt-spinning under argon atmosphere onto a copper wheel with a surface speed of 39 m/s. The crystallized  $\text{Ni}_{50}\text{Nb}_{50}$  samples were obtained by annealing the amorphous ribbons in vacuum ( $\sim 10^{-4}$  Pa) at certain temperatures with heating and cooling rates of 0.33 K/s. The temperatures for heat treatments were chosen based on the crystallization reaction measured by differential scanning calorimetry (DSC). Thermal stability of  $\text{Ni}_{50}\text{Nb}_{50}$  amorphous ribbons was analyzed in a Netzsch DSC 404C under purified flowing argon at a heating rate of 0.33 K/s. The as-quenched and annealed samples were examined by X-ray diffraction (XRD) using a Rigaku D/max 2400 diffractometer (Tokyo, Japan) with monochromated Cu K $\alpha$  radiation ( $\lambda = 0.1542$  nm). An FEI Tecnai F30 transmission electron microscope (TEM) was used to confirm the microstructure of as-quenched and annealed alloys. The thin foils for TEM observations were prepared by a standard twin-jet electro-polishing method in a bath of 10%  $\text{H}_2\text{SO}_4$  in methanol at 253 K [21].

Electrochemical measurements of the as-quenched and annealed samples were conducted on a potentiostat–galvanostat EG&G Princeton Applied Research model 273 in a three electrode cell with a platinum counter electrode and a saturated calomel reference electrode (SCE). Only free sides of the ribbons were treated as working electrode and grinded with 1500-grits SiC papers followed by ethanol cleansing. The surface roughness of both amorphous and crystallized samples after mechanical grinding was analyzed by a MicroXAM-3D non-contact profiler system. The wheel sides of the ribbons and the undesired areas were sealed by a mixture of paraffin and colophony, leaving a grinded surface for electrochemical testing. Potentiodynamic or cyclic polarization curves were measured with a potential sweep rate of 0.33 mV/s in 1 mol/L HCl aqueous solution after immersing the samples for several minutes when the open-circuit potential became almost steady. Potentiostatic measurements were evaluated on a working electrode with an area of 1 mm<sup>2</sup> at the polarization potentials of 0.8, 1.0 and 1.2 V (SCE) in 1 mol/L HCl solution for 10<sup>4</sup> s. The samples were immersed in HCl solution for 1000 s just prior to the potentiostatic measurements. The current during potentiostatic measurements was recorded continuously by the computer with a current detection limit of about 0.1 nA. All the electrochemical tests were held at 298 K in a water bath. The potentials mentioned in this paper are all referred to SCE.

The surface morphologies of the samples before and after corrosion were characterized by an atomic force microscopy (Picoplus 2500 AFM, Molecular Imaging Corp.) in tapping mode using cantilever with linear tips. Both the amorphous and crystallized samples for AFM observation were carefully polished with 0.5  $\mu\text{m}$  alumina powders and ultrasonically cleaned in acetone. The

samples for corrosion were then sealed carefully as mentioned above to perform potentiostatic polarization tests at 1.0 V (SCE) for 10<sup>4</sup> s. After potentiostatic tests, the samples were again ultrasonically cleaned in acetone ( $\sim 30$  min each time) for three times to remove any contaminations at the surface.

The surface film was analyzed by X-ray photoelectron spectroscopy (XPS) using an ESCALAB250 photoelectron spectrometer with Al K $\alpha$  excitation ( $h\nu = 1486.6$  eV). The spot area for testing is randomly selected at the surface with a diameter of 0.5 mm. Binding energies were calibrated using the carbon contamination with C 1s peak value of 284.6 eV. The depth profiles of the alloy surface were characterized by *in situ* XPS ion beam sputtering with 2 kV, 2  $\mu\text{A}$  argon ions at a sputtering rate of about 0.2 nm/s.

## 3. Results

### 3.1. As-quenched structure and crystallization reaction

Fig. 1 shows XRD patterns of the free and wheel surfaces of the as-quenched  $\text{Ni}_{50}\text{Nb}_{50}$  ribbons. Only a main halo peak without crystalline peaks is determined, indicating a single glassy phase formed in these samples. Upon heating, there exhibits only one distinct exothermic reaction at 973 K in this alloy (see inset of Fig. 1). To ascertain the crystallization product, the samples were annealed ranging from 933 to 993 K for 30 min and 1073 K for 260 min, respectively. Only an M-phase can be determined in these annealed samples (see Fig. 2), which is in a good agreement with the M-phase reported in Refs. [21–23]. Previous studies have shown that the M-phase was very stable at lower temperatures but would transform to the equilibrium phase NiNb after annealing at high temperatures (1050–1100 K) [21]. However, in our tests, no such transformation from M-phase to NiNb-phase occurs after the sample annealing at 1073 K for 260 min. From Fig. 2, it is noted that the M-phase partially precipitates from amorphous matrix at relatively low annealing temperature (around 933 K), but the crystallization reaction tends to be finished upon sample heating up to 953 K for 30 min. This result has further confirmed that the  $\text{Ni}_{50}\text{Nb}_{50}$  metallic glass undergoes single M-phase polycrystallization reaction during devitrification.

To ascertain the microstructure of the as-quenched and annealed  $\text{Ni}_{50}\text{Nb}_{50}$  samples, the specimens were examined with TEM. No second phase can be detected in the as-quenched specimens. High-resolution TEM observations, as shown in Fig. 3a, confirm their fully amorphous structure nature. Fig. 3b illustrates the

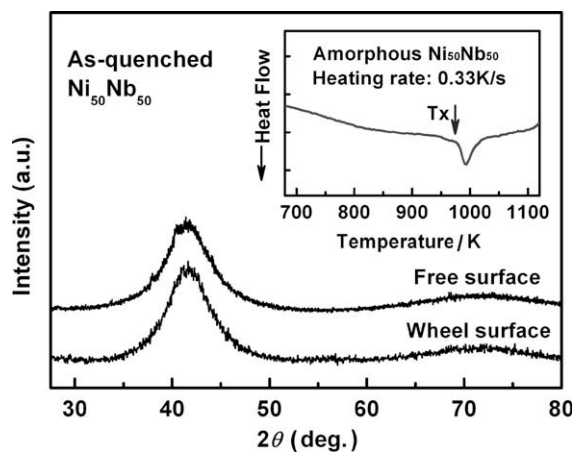


Fig. 1. X-ray diffraction patterns of both free and wheel surfaces of the as-quenched  $\text{Ni}_{50}\text{Nb}_{50}$  ribbon and the differential scanning calorimetry (DSC) curve for  $\text{Ni}_{50}\text{Nb}_{50}$  metallic glass.

Download English Version:

<https://daneshyari.com/en/article/1471005>

Download Persian Version:

<https://daneshyari.com/article/1471005>

[Daneshyari.com](https://daneshyari.com)